

Dynamics of phenyl-based polymer chains confined in thin layers

DISSERTATION

for the attainment of the academic degree

Bachelor of Science

at the

International Physics Study Program (IPSP) of the University of Leipzig

submitted by

Federico Porcelli

born on 16.03.2001 in Bisceglie

prepared in the
IPSP Leipzig

Supervised by

Dr. Martin Treß

Decision on the conferral of the bachelor degree dated 15.09.2024

Contents

0.1	Bibliography	1
0.2	List of Abbreviations	2
1	Introduction	3
2	Theoretical Background	5
2.1	Basic Concepts	5
2.1.1	Maxwell's Equations	5
2.1.2	Electric Displacement Field	5
2.1.3	Complex Dielectric Function	6
2.1.4	Dielectric Relaxation	6
2.2	Relaxation in Polymers	7
2.3	Thin Films	7
2.3.1	Introduction to Thin Films	7
2.3.2	Dynamics in Thin Films	7
2.3.3	Two Different Interpretations	7
2.4	Modeling Functions	7
2.4.1	Expanding on the Debye Model	7
2.4.2	The Havriliak-Negami Function	8
2.5	The Derivative Method	8
2.5.1	Our Fitting Function	9
3	Methods & Materials	11
3.1	The Polymers in Question	11
3.1.1	Poly-TPD	11
3.1.2	Poly-Bisphenol	11
3.2	Preparation of the samples	12
3.2.1	Solution Preparation	12
3.2.2	Preparation of the Substrate	12
3.2.3	Spin-Coating of the Solution	13
3.2.4	Heating and Annealing	13
3.3	Atomic Force Microscopy	13
3.4	Dielectric Spectroscopy	14
4	Results & Discussion	15
4.1	Obtained Dielectric Spectra	15
4.1.1	Qualitative Observations	15
4.2	Fitting of the Data	17
4.3	Discussion about the Obtained Parameters	17
4.3.1	Relaxation Times	17
4.3.2	Dielectric strengths ($\Delta\epsilon$)	17
4.3.3	β/γ ?	17

0.1 Bibliography

Federico Porcelli

Dynamics of phenyl-based polymer chains confined in thin layers

Universität Leipzig, Dissertation

21 pages, 7 figures, 1 attachments

0.2 List of Abbreviations

Poly-TPD Poly([N,N'-diphenyl-N,N'-bis(4-tert-butylphenyl)-(1,1'-biphenyl)-4,4'-diamine]-alt-formaldehyde)

Poly-Bisphenol 4,4-Dihydroxydiphenyl-2,2-propane carbonate polymer

DF dielectric function

TPD triarylamine

HN Havriliak-Negami

EP electrode polarization

FA fluorene

OPV organic photovoltaic

OLED organic light-emitting diode

HTL hole transport layer

GPC gel permeation chromatography

BDS broadband dielectric spectroscopy

RMS root mean square

KK Kramers-Kronig

Chapter 1

Introduction

In bulk polymers, physical properties such as heat capacity, thermal expansion coefficient, dielectric permittivity, and refractive index are well-defined and uniform. Studies of the glass transition in bulk polymers typically involve measuring changes in these parameters as a function of time or temperature. However, when polymers are confined to thin films, the situation changes significantly. The glassy dynamics near the interfaces alter, leading to variations in properties like dielectric permittivity, thermal expansion, heat capacity, and refractive index within the film. Unlike bulk materials, thin polymer films exhibit a heterogeneous response due to the complex interplay of these local variations. Consequently, measurements on thin films reflect a collective response that averages multiple local contributions.

The present work aims to illustrate how these contributions combine to produce the overall dielectric response of thin polymer films, particularly through broadband dielectric spectroscopy. The focus will be on two polymers in particular, namely Poly-TPD, studied for its superior charge transport properties in organic electronics, and P-Bisphenol, valued for its high thermal stability and mechanical strength in engineering applications.

Chapter 2

Theoretical Background

2.1 Basic Concepts

2.1.1 Maxwell's Equations

Maxwell's equations form the foundation of classical electromagnetism, describing how electric charges and currents produce electric and magnetic fields, as well as how those fields interact with each other and with matter. It is deemed worthwhile to quickly recall them:

1. **Gauß Theorem for Electricity:**

$$\nabla \cdot \mathbf{E} = \frac{\rho}{\epsilon_0} \quad (2.1)$$

2. **Gauß Theorem for Magnetism:**

$$\nabla \cdot \mathbf{B} = 0 \quad (2.2)$$

3. **Faraday's Law of Induction:**

$$\nabla \times \mathbf{E} = -\frac{\partial \mathbf{B}}{\partial t} \quad (2.3)$$

4. **Ampère's Law (with Maxwell's addition):**

$$\nabla \times \mathbf{B} = \mu_0 \mathbf{J} + \mu_0 \epsilon_0 \frac{\partial \mathbf{E}}{\partial t} \quad (2.4)$$

2.1.2 Electric Displacement Field

The electric displacement field \mathbf{D} relates to the electric field \mathbf{E} and the polarization \mathbf{P} within a medium. It accounts for both free and bound charges in the material and is defined by the equation:

$$\mathbf{D} = \epsilon_0 \mathbf{E} + \mathbf{P} = \epsilon_0 \epsilon \mathbf{E}$$

where ϵ_0 is the permittivity of free space, \mathbf{E} is the electric field, \mathbf{P} is the polarization vector (i.e. dipole moment per unit volume of the material), and ϵ represents the dielectric function (DF) and is generally a tensor of rank 2 because of the non-required collinearity between \mathbf{D} and \mathbf{E} .

2.1.3 Complex Dielectric Function

In most instances though, ϵ will be treated as a complex (scalar) function $\epsilon^*(\omega)$, which varies with frequency due to the contributions of different oscillators in the analyzed materials. Namely it's given by:

$$\epsilon^* = \epsilon' + i\epsilon''$$

where the complex ϵ'' and the real ϵ' parts are related by the Kramers-Kronig relation.

2.1.4 Dielectric Relaxation

The dielectric relaxation theory for small electric field strengths is a specific application of linear response theory, applicable to isotropic systems. In this context, the time-dependent response $y(t)$ of a system, following a disturbance $x(t)$, is described by a linear equation. For dielectrics, the disturbance is the time-dependent external electric field $x(t) = E(t)$, and the response is the polarization $y(t) = P(t)$. This relationship is given by:

$$P(t) = P_\infty + \epsilon_0 \int_{-\infty}^t \epsilon(t-t') \frac{dE(t')}{dt'} dt'$$

where $\epsilon(t)$ is the time-dependent dielectric function, and P_∞ includes all contributions from induced polarization. This equation relies on the principles of linearity (the system's response to multiple disturbances is the sum of individual responses) and causality (only past disturbances influence the response at time t).

When a stationary periodic electric field $E(t) = E_0 e^{-i\omega t}$ is applied, the equation transforms to:

$$P(t, \omega) = \epsilon_0 (\epsilon^*(\omega) - 1) E(t, \omega)$$

with the complex dielectric function defined as:

$$\epsilon^*(\omega) = \epsilon'(\omega) - i\epsilon''(\omega)$$

Here, $\epsilon'(\omega)$ represents the energy stored in the system per period, and $\epsilon''(\omega)$ corresponds to the energy dissipated per period. The relationship between the time-dependent dielectric function $\epsilon(t)$ and the complex dielectric function $\epsilon^*(\omega)$ is given by:

$$\epsilon^*(\omega) = \epsilon_\infty - \int_0^\infty \frac{d\epsilon(t)}{dt} e^{-i\omega t} dt$$

This expression is a one-sided Fourier or full imaginary Laplace transformation.

2.2 Relaxation in Polymers

2.3 Thin Films

2.3.1 Introduction to Thin Films

2.3.2 Dynamics in Thin Films

2.3.3 Two Different Interpretations

2.4 Modeling Functions

When we aim to analyze dielectric spectra, it all comes down to give physical models that give insight into the occurring phenomena. A simple, commonly-used approximation is the model of relaxation time. The most general way to understand it is that the time derivative of a quantity is proportional to the quantity itself. As an instance:

$$\frac{dP(t)}{dt} = -\frac{P(t)}{\tau_D}$$

where τ_D is the characteristic relaxation time. Solving this equation yields an exponential decay for the correlation function $\Phi(\tau)$:

$$\Phi(\tau) = \exp\left(-\frac{\tau}{\tau_D}\right)$$

This leads to the following complex dielectric function $\epsilon^*(\omega)$:

$$\epsilon^*(\omega) = \epsilon_\infty + \frac{\Delta\epsilon}{1 + i\omega\tau_D} \quad (2.5)$$

where $\Delta\epsilon = \epsilon_S - \epsilon_\infty$ is the dielectric relaxation intensity, with $\epsilon_S = \lim_{\omega \rightarrow 0} \epsilon'(\omega)$ and $\epsilon_\infty = \lim_{\omega \rightarrow \infty} \epsilon'(\omega)$.

The Debye relaxation time τ_D is related to the position of maximal loss by

$$\omega_p = \frac{2\pi}{\nu_p} = \frac{1}{\tau_D} \quad (2.6)$$

Equation 2.5 is known as Debye relaxation, and is the basis for further models we will discuss next.

2.4.1 Expanding on the Debye Model

The Debye model above is, however, not sufficient to describe all the effects that happen within the dielectric spectra in most cases. Therefore, non-Debye models have been introduced, and a short outline will be discussed below.

A commonly used model is the Cole-Cole function, given by:

$$\epsilon_{CC}^*(\omega) = \epsilon_\infty + \frac{\Delta\epsilon}{1 + (i\omega\tau_{CC})^\beta}$$

where $0 < \beta \leq 1$. This function introduces a symmetrical broadening of the relaxation function, with the Debye function recovered when $\beta = 1$. The characteristic relaxation time τ_{CC} determines the position of maximal loss, defined analogously as in Equation 2.6.

For cases where the dielectric function exhibits asymmetric broadening, the Fuoss-Kirkwood or Cole-Davidson functions are more appropriate. The Cole-Davidson function is expressed as:

$$\epsilon_{\text{CD}}^*(\omega) = \epsilon_{\infty} + \frac{\Delta\epsilon}{(1 + i\omega\tau_{\text{CD}})^{\gamma}}$$

Here, $0 < \gamma \leq 1$ introduces asymmetry, with the Debye function being a special case when $\gamma = 1$. The characteristic relaxation time τ_{CD} does not necessarily correspond to the position of maximal loss, which is instead given by:

$$\omega_p = \frac{1}{\tau_{\text{CD}}} \tan\left(\frac{\pi}{2\gamma + 2}\right)$$

2.4.2 The Havriliak-Negami Function

A more general approach is provided by the Havriliak-Negami (HN) function, which combines features of both the Cole-Cole and Cole-Davidson functions:

$$\epsilon_{\text{HN}}^*(\omega) = \epsilon_{\infty} + \frac{\Delta\epsilon}{(1 + (i\omega\tau_{\text{HN}})^{\beta})^{\gamma}}$$

In the HN function, $0 < \beta, \gamma \leq 1$, where β and γ describe the symmetric and asymmetric broadening, respectively. The behavior of the dielectric function at low and high frequencies, $\epsilon_s - \epsilon'(\omega) \sim \omega^m$ and $\epsilon'' \sim \omega^m$ for $\omega \ll 1/\tau_{\text{HN}}$, is characterized by the exponent $m = \beta$.

The dielectric function's behavior at high frequencies can be described by the following relationships:

$$\epsilon'(\omega) - \epsilon_{\infty} \sim \omega^{-n} \quad \text{and} \quad \epsilon'' \sim \omega^{-n} \quad \text{for} \quad \omega \gg \frac{1}{\tau_{\text{HN}}}$$

with $n = \beta\gamma$. The parameters m and n , introduced by Jonscher, represent the slopes of $\log \epsilon''$ versus $\log \omega$ at low and high frequencies, respectively, relative to the position of maximal loss.

The position of maximal loss ω_p depends on the shape parameters β and γ as follows:

$$\omega_p = \frac{1}{\tau_{\text{HN}}} \left[\sin\left(\frac{\beta\pi}{2 + 2\gamma}\right) \right]^{\frac{1}{\beta}} \left[\sin\left(\frac{\beta\gamma\pi}{2 + 2\gamma}\right) \right]^{-\frac{1}{\beta}}$$

and therefore,

$$\tau_c(\beta, \gamma) = \tau_{\text{HN}} \left[\sin\left(\frac{\pi\beta\gamma}{2 + 2\gamma}\right) \right]^{-\frac{1}{\beta}} \left[\sin\left(\frac{\pi\beta}{2 + 2\gamma}\right) \right]^{\frac{1}{\beta}}$$

corresponds to the relaxation time at maximum loss peak.

2.5 The Derivative Method

Due to the significant conductivity contribution, which obscures the clear observation of the loss peak near the glass transition temperature, the derivative method has to be employed. This consists in exploiting the Kramers-Kronig (KK) relation to our advantage: since the integral transform of ϵ' doesn't include the (ionic) Ohmic conduction term, it will contain the same information as ϵ'' without this conductivity contribution.

An easy way to interpret ϵ' is to take its derivative and using the relationship:

$$\epsilon''_{\text{der}} = \left(-\frac{\pi}{2}\right) \frac{d\epsilon'}{d \ln f} \approx \epsilon''_{\text{rel}}$$

which means that the HN function for the derivative of ϵ' will have the form:

$$\frac{\partial \epsilon'_{\text{HN}}}{\partial \ln f} = -\frac{\beta \gamma \Delta \epsilon \cdot (2\pi f \tau)^\beta \cos\left[\beta \frac{\pi}{2} - (1 + \gamma)\theta_{\text{HN}}\right]}{\left[1 + 2(2\pi f \tau)^\beta \cos\left(\frac{\beta \pi}{2}\right) + (2\pi f \tau)^{2\beta}\right]^{(1+\gamma)/2}}$$

where

$$\theta_{\text{HN}} = \arctan\left[\frac{\sin(\pi\beta/2)}{(2\pi f \tau)^{-\beta} + \cos(\pi\beta/2)}\right]$$

and the rest of the parameters are defined as before.

2.5.1 Our Fitting Function

Based on these considerations, the fitting function for our data will have the following form:

$$F(\Delta\epsilon_i, \tau_{\text{HN}_i}, \beta_i, \gamma_i, \sigma_0, a) = \sum_{i=1}^3 \left(\frac{\partial \epsilon'_{\text{HN}}}{\partial \ln f} \right)_i + \frac{\sigma_0}{\epsilon_0 \omega^a}$$

where the first term consists in multiple HN functions which are summed together – up to three, depending on the number of peaks in the spectrum – and the second term indicates the electrode polarization (EP), which usually happens at low frequencies before the first HN peak, and has the form of a DC conductivity, but is not always occurring and thus optional.

Chapter 3

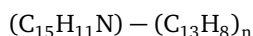
Methods & Materials

3.1 The Polymers in Question

Two different polymers are analyzed in this work: Poly([N,N'-diphenyl-N,N'-bis(4-tert-butylphenyl)-(1,1'-biphenyl)-4,4'-diamine]-alt-formaldehyde) (Poly-TPD) and 4,4-Dihydroxydiphenyl-2,2-propane carbonate polymer (Poly-Bisphenol).

3.1.1 Poly-TPD

Poly-TPD is from the supplier Polymer Source, Inc.™ with the sample number P16210-PolyTPD-FA, has a $M_n = 28.500$, and $M_w = 32.000$. It consists of triarylamine (TPD) with fluorene (FA) units incorporated into its backbone. The chemical structure can be described by the repeating units:

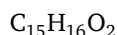


This polymer contains an FA conjugated backbone that is critical for its semiconducting properties. In particular its high hole mobility, in the range of 10^{-4} to 10^{-3} cm^2/Vs , makes it suitable for use as a hole transport layer (HTL) in organic light-emitting diode (OLED) and organic photovoltaic (OPV) devices.

As for its thermodynamic properties, Poly-TPD exhibits good thermal stability, with a decomposition temperature $T_d > 350^\circ\text{C}$, and a glass transition temperature around $90\text{-}150^\circ\text{C}$.

3.1.2 Poly-Bisphenol

Poly-Bisphenol, on the other hand, came from the manufacturer Sigma-Aldrich, with the sample code 181625-250G Poly(Bisphenol A carbonate), and has a $M_w \approx 45.000$ by gel permeation chromatography (GPC). Its glass transition temperature is $T_g \approx 150^\circ\text{C}$, and melting point $T_m \approx 267^\circ\text{C}$. It has the repeating unit (or monomer)



and is a thermoplastic polymer with optical clarity, high tensile strength/impact resistace, high refractive index, and it is used, for example, to prepare optical lenses or as a supporting matrix to fabricate hybrid nanofiber membranes.

3.2 Preparation of the samples

The preparation of the samples required for our analysis involves creating parallel-plate capacitors on a glass substrate. These capacitors have an area of approximately 6×6 mm and a thickness that varies from around 300 nm to 5 nm.

Controlling the thickness of the dielectric material within the capacitor is particularly important, as our goal is to study the effects of thin layers compared to the bulk material. This control is achieved by preparing polymer solutions with different concentrations: the higher the concentration, the thicker the resulting film.

3.2.1 Solution Preparation

In particular, 7 solutions were prepared for each of the polymers starting from a concentration of 20 mg/ml and roughly halvened. The solvent used for Poly-TPD was Chloroform, while Poly-Bisphenol was diluted in Dichloromethane.

As an example, to compute the volume required to dilute a solution from an initial concentration of 20 mg/ml to a desired concentration of 10 mg/ml, with a final volume of 10 ml, we use the dilution formula:

$$C_1 V_1 = C_2 V_2$$

where:

$$C_1 = 20 \text{ mg/ml} \quad (\text{initial concentration})$$

$$C_2 = 10 \text{ mg/ml} \quad (\text{desired concentration})$$

$$V_1 = \text{unknown volume (to be calculated)}$$

$$V_2 = 10 \text{ ml} \quad (\text{final volume})$$

Substituting the known values:

$$20 \text{ mg/ml} \times V_1 = 10 \text{ mg/ml} \times 10 \text{ ml}$$

Solving for V_1 :

$$V_1 = \frac{10 \text{ mg/ml} \times 10 \text{ ml}}{20 \text{ mg/ml}} = \frac{100 \text{ ml}}{20} = 5 \text{ ml}$$

This was done similarly for all other solutions, and the resulting concentrations are shown in Table 3.1

3.2.2 Preparation of the Substrate

The glass substrates were prepared by cutting standard microscope slides into approximately 1×1 cm squares, followed by cleaning in an ultrasonic cleaner using ethanol and deionized water. This cleaning process ensures a contaminant-free surface for the deposition of polymer solutions. After cleaning, the substrates were dried using pressurized N_2 in a laminar flow hood to avoid dust contamination and then stored in a Petri dish.

Once the substrates were prepared, the next step was to create the first of the two plates of the capacitors. This was accomplished by depositing gaseous aluminum in approximately 5 mm wide strips across the substrate. Specifically, to produce a total of 9 capacitors, three equally spaced strips of aluminum were deposited. This was done using a complementary mask, which covered all areas of the substrate except for where the strips were intended to be, ensuring that the evaporated aluminum only adhered to the exposed glass surface.

Table 3.1: Concentrations and volumes of both sets of solutions (Poly-TPD and P-Bisphenol)

C (mg/ml)	$V_{solution}$ (ml)	$V_{solvent}$ (ml)
10	5	5
3	3	7
1	3	6
0.5	4	4
0.2	4	6
1	5	5

The thermal evaporation process used for this deposition is relatively straightforward. It involves melting a small quantity of aluminum (in our case, taken from tiny cut wire) in a turbomolecular-pump vacuum chamber by heating a tungsten base with a high current. This results in the desired evaporation of the metal and its subsequent surface accumulation. The thickness of this accumulation can be controlled by adjusting the duration of the current applied to the tungsten base. In our case, just a few seconds of heating produced an aluminum layer approximately 200 nm thick.

3.2.3 Spin-Coating of the Solution

Once the first of the two aluminum capacitor plates is deposited on the glass substrate, the next step is to apply the dielectric material between the plates. This is achieved by depositing the respective polymer solution onto the plate. The spin-coating technique is particularly useful in this case, as it ensures a uniform distribution of the solution across the glass layer.

In our procedure, a spin-coating program of 1 minute at 4000 rpm was used for all polymer solutions to ensure reproducibility.

Moreover, the glass slides were marked appropriately to allow for distinction of polymer and concentration at a later time.

3.2.4 Heating and Annealing

After spin-coating the solution, the samples were placed in a small glass container, which was then evacuated to remove any trapped air or moisture. The container was subsequently placed inside an oven set to 200°C and maintained at this temperature for 12 hours to allow for annealing.

Annealing is useful for improving the film's uniformity and adhesion to the substrate, enhancing its mechanical properties, and promoting the removal of residual solvents. It also helps in stabilizing the polymer film by allowing the polymer chains to rearrange and settle into a more stable configuration.

After this process, aluminum was evaporated a second time in strips perpendicular to the earlier ones, completing the fabrication of the capacitors.

3.3 Atomic Force Microscopy

The use of Atomic Force Microscopy (AFM) is particularly useful when measuring the thickness of the dielectric in our samples. This measurement is essential due to the capacitance formula for a

parallel-plate capacitor:

$$C = \epsilon \frac{A}{d}$$

where ϵ is the permittivity, A is the surface area of the plate, and d is its thickness. Since dielectric measurements rely on this formula, both A and d must be accurately determined. The former is a straightforward parameter to obtain, and in our case, it was measured using a simple optical microscope.

The measurement of the latter, however, is more challenging and cannot be obtained by the initial concentration of the spin-coated solution, as this would be overly imprecise and unreliable.

To accurately determine the thickness, AFM is employed in the following manner:

1. The surface of the sample is first scratched with a needle in a non-capacitor region (i.e., where no aluminum is present) as shown in the figure. This scratch allows for the measurement of the thickness of the deposited polymer layer.
2. The scratched area is then positioned under the AFM tip, with approximately half of the scratched region occupying the field of view and the non-scratched region occupying the other half.
3. This setup allows for the measurement of the relative height between the substrate and the polymer film, which is then analyzed using Gwyddion, where a simple statistical average of the two heights can be calculated, providing a relatively accurate thickness of the dielectric.

This process was repeated two or more times for each sample, and the resulting thicknesses were then averaged for each of the capacitors. The results of these measurements are presented below.

3.4 Dielectric Spectroscopy

Once we know the parameters of our samples, we can move to the actual broadband dielectric spectroscopy (BDS) measurements. This technique enables to obtain (among other things) the frequency and temperature-dependent complex and real parts of the DF ϵ^* , from which molecular dipole dynamics, polarization phenomena, and relaxation processes can be deduced. In our case, the frequency range was set up to be from 10^{-1} Hz to 10^6 Hz, and a temperature from about 290K to 530K.

A frequency generator takes care of the AC current input, with a root mean square (RMS) voltage $V_{RMS} = 0.1$ V, while temperature is controlled using a Dewar flask containing liquid nitrogen, and resistances that are heated depending on the wanted temperature. The temperature of the sample is then measured using a platinum resistance thermometer, which allows for a very precise sensing of T (with an error of less than 1K).

Proper attention must be given to the connection between the sample and the BDS setup. This is achieved by using copper/gold terminals that are secured to the aluminum surface of the capacitor plates with screws, ensuring firm contact with the glass slide. Careful attention is given to ensure that the resistance is less than 2Ω across the plate and the BDS terminals, and $> 20M\Omega$ between the two plates (otherwise it would be counted as a shorted capacitor).

That done, the sample holder is placed in the setup and the measurement can be started, lasting about 18 hours for the whole temperature range to be recorded on both heating and cooling, such that reproducibility is guaranteed. However, especially in thinner films, it was noted that the sample undergoes some dielectric changes after being exposed to rapid and repeated temperature fluctuations.

Chapter 4

Results & Discussion

4.1 Obtained Dielectric Spectra

The final dielectric spectra are plotted in Figures 4.1, 4.2, 4.3 and 4.4 for the various thicknesses of Poly-TPD and 4.5, 4.6 and 4.7 for Poly-Bisphenol, along with the derivative of epsilon prime.

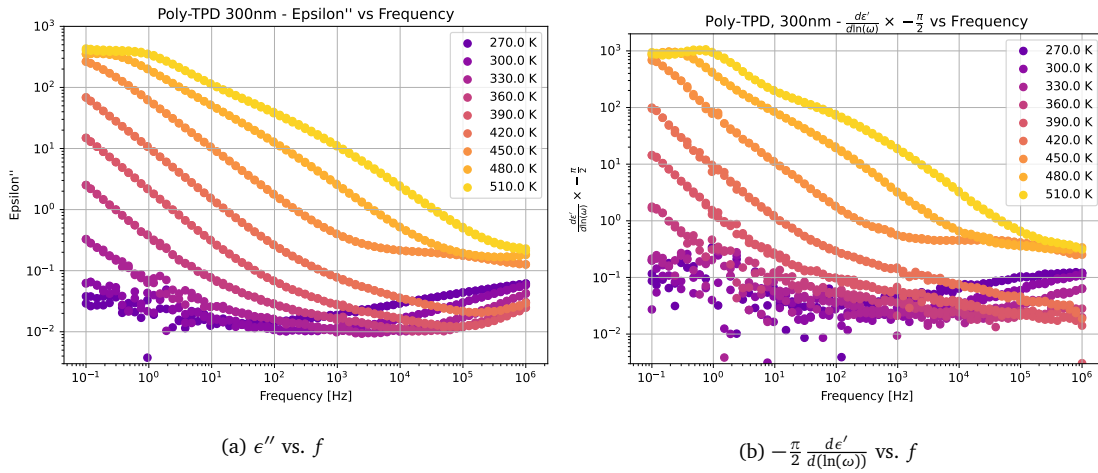


Figure 4.1: 300nm Poly-TPD thin film, complex dielectric function and derivative of the real part as a function of frequency at different temperatures (plotted once every 30 kelvin for clarity).

4.1.1 Qualitative Observations

A quick overview at the obtained spectra brings one to notice the following traits:

- The derivative plot is generally more helpful in identifying the occurring peaks, which are more pronounced with respect to the ϵ'' plot. This happens because of the removal of Ohmic conductivity, as discussed earlier.
- At low temperature, the plots become more imprecise, probably due to a combination of the electronic oscillations and computation artifacts in the case of the derivative. In some cases, a spline interpolation was used to make the data more suitable for the subsequent fitting.

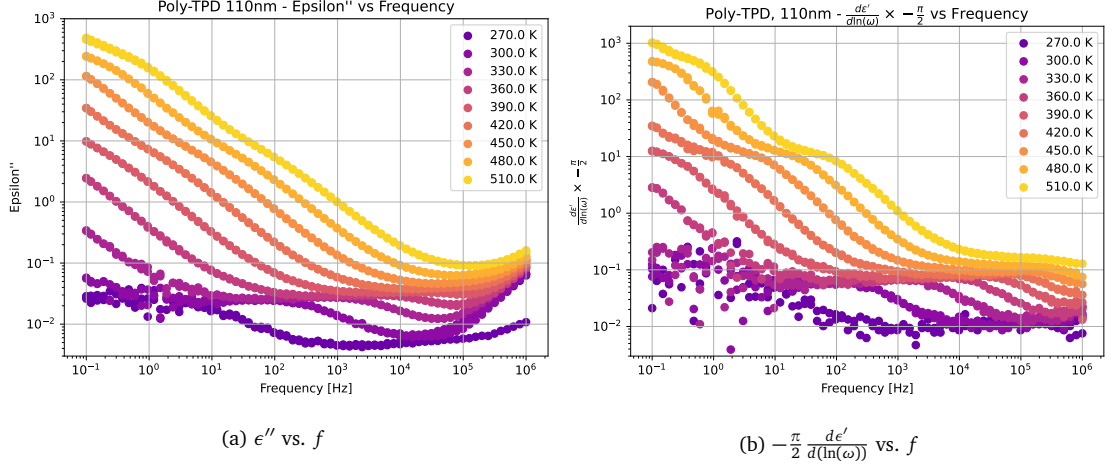


Figure 4.2: 110nm Poly-TPD thin film

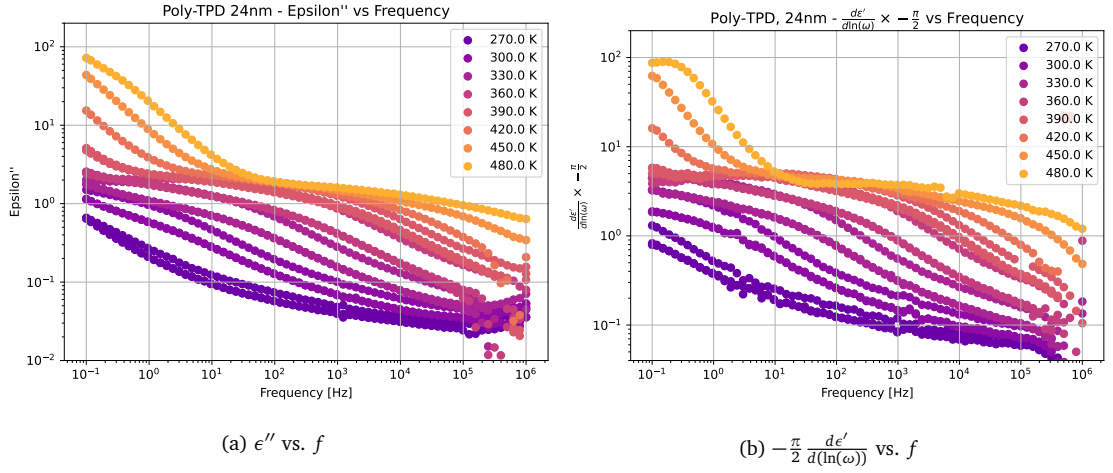


Figure 4.3: 24nm Poly-TPD thin film

- Thinner films generally exhibit a breakdown (i.e. shorting) at lower temperatures, although not always (as was the case of the 320nm Poly-Bisphenol film). This is consistent with the expectation that higher temperatures facilitate the penetration of the aluminum layers in the polymer, which becomes more conductive and eventually shorted. Also the thermal expansion of aluminum might be playing a role, though it should only be relevant for the thinner films, as its range of action is $\approx 5\text{nm}$.

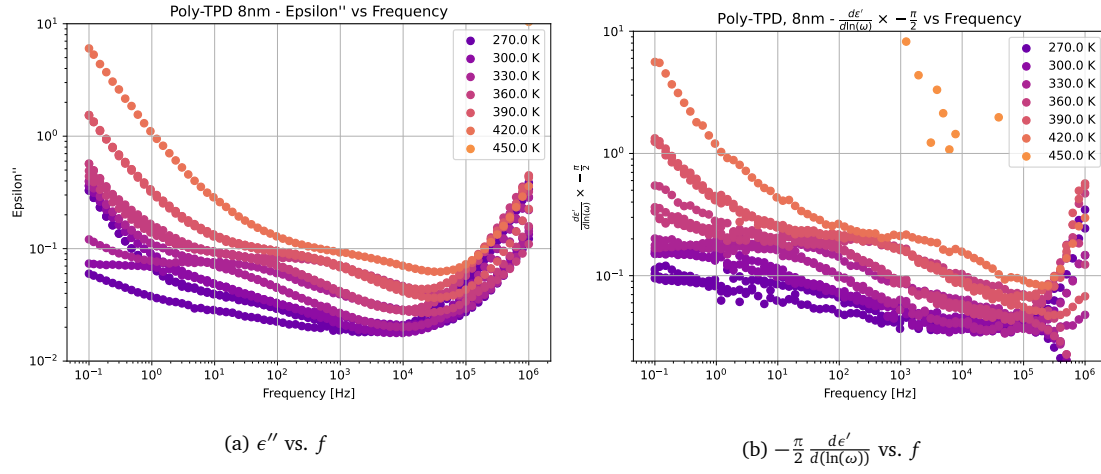


Figure 4.4: 8nm Poly-TPD thin film

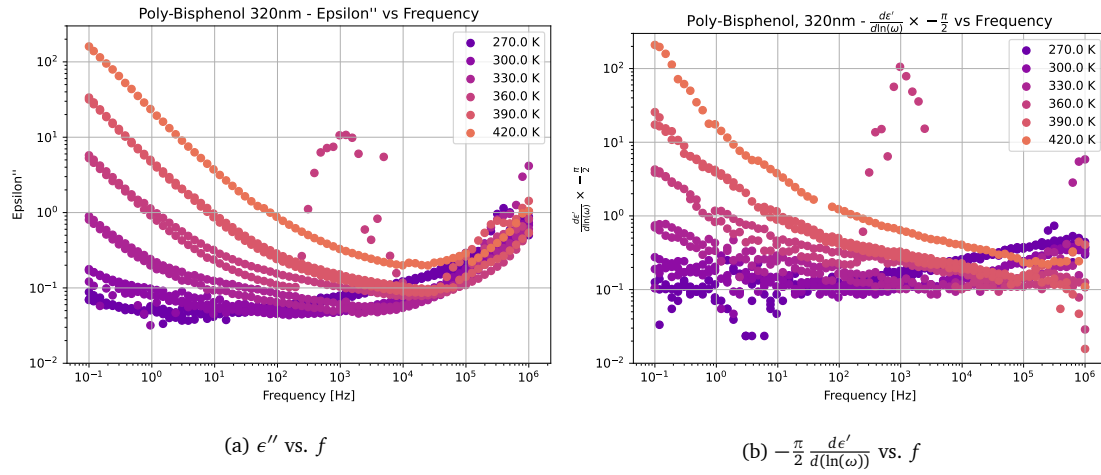


Figure 4.5: 320nm Poly-Bisphenol thin film

4.2 Fitting of the Data

4.3 Discussion about the Obtained Parameters

4.3.1 Relaxation Times

VFT fit of the relaxation times

Discussion and Comparison with other Polymers in Literature

4.3.2 Dielectric strengths (Delta Epsilon)

4.3.3 beta/gamma?

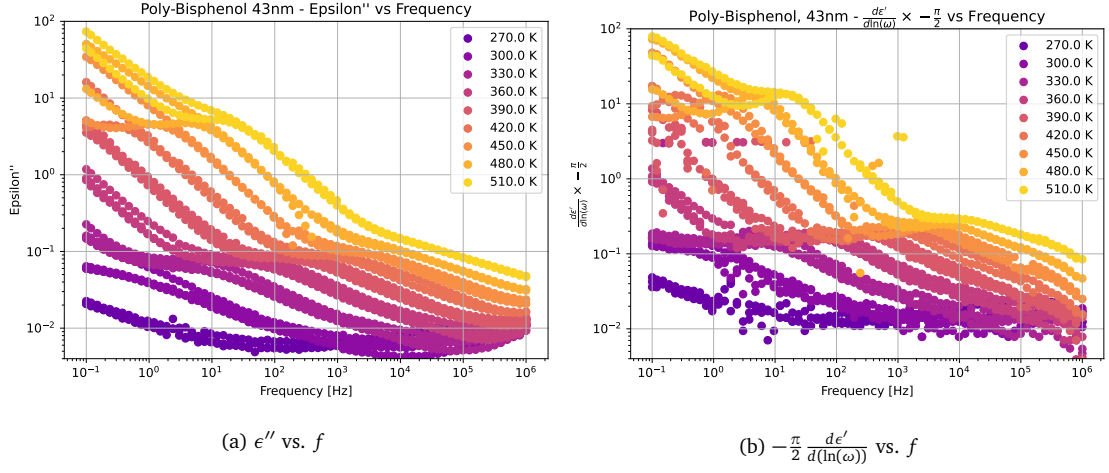


Figure 4.6: 43nm Poly-Bisphenol thin film

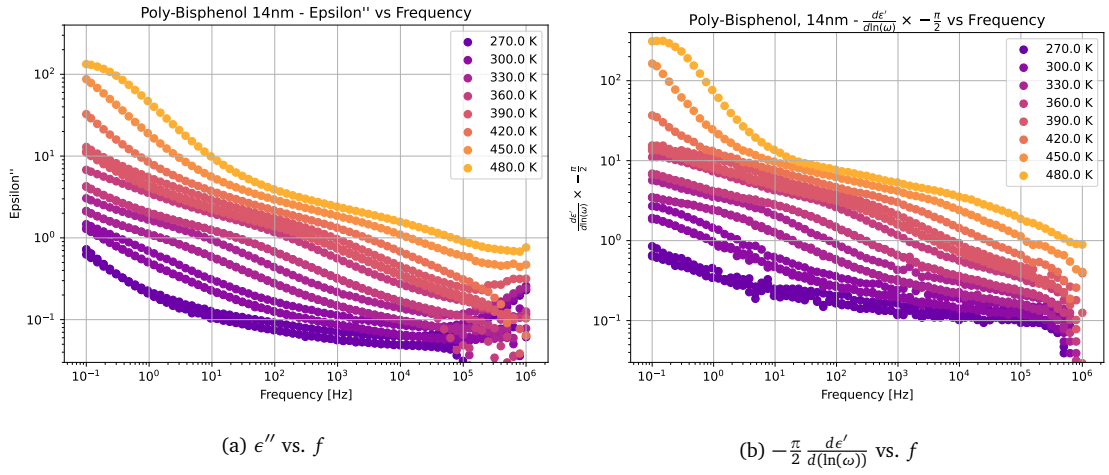


Figure 4.7: 14nm Poly-Bisphenol thin film

Chapter 5

Synopse

Dissertation for the attainment of the academic degree:
Bachelor of Science

Dynamics of phenyl-based polymer chains confined in thin layers

submitted by:
Federico Porcelli

prepared in:
IPSP Leipzig

supervised by:
Dr. Martin Treß

September 2024

Lorem ipsum dolor sit amet, consectetur adipiscing elit. Etiam lobortis facilisis sem. Nullam nec mi et neque pharetra sollicitudin. Praesent imperdiet mi nec ante. Donec ullamcorper, felis non sodales commodo, lectus velit ultrices augue, a dignissim nibh lectus placerat pede. Vivamus nunc nunc, molestie ut, ultricies vel, semper in, velit. Ut porttitor. Praesent in sapien. Lorem ipsum dolor sit amet, consectetur adipiscing elit. Duis fringilla tristique neque. Sed interdum libero ut metus. Pellentesque placerat. Nam rutrum augue a leo. Morbi sed elit sit amet ante lobortis sollicitudin. Praesent blandit blandit mauris. Praesent lectus tellus, aliquet aliquam, luctus a, egestas a, turpis. Mauris lacinia lorem sit amet ipsum. Nunc quis urna dictum turpis accumsan semper.

Declaration of Independent Work

I hereby declare that I have completed the present work independently and without any unauthorized assistance or use of sources other than those specified. I affirm that no third party has received any monetary compensation from me, either directly or indirectly, for work related to the content of this dissertation, and that the submitted work has not been presented in the same or a similar form to any other examination authority, either domestically or abroad, for the purpose of obtaining a degree or other certification. All material taken from other sources or from other individuals that has been used in this work or directly referenced has been clearly marked as such. In particular, all individuals who directly contributed to the creation of this work have been acknowledged.

Leipzig, September 2, 2024

Federico Porcelli